The peroxisomal membrane protein import receptor Pex3p is directly transported to peroxisomes by a novel Pex19p- and Pex16p-dependent pathway

Takashi Matsuzaki[1] and Yukio Fujiki[1,2]

[1]Department of Biology, Faculty of Sciences, Kyushu University Graduate School, Fukuoka 812-8581, Japan
[2]Core Research for Evolutional Science and Technology, Japan Science and Technology Agency, Chiyoda, Tokyo 102-0075, Japan

Two distinct pathways have recently been proposed for the import of peroxisomal membrane proteins (PMPs): a Pex19p- and Pex3p-dependent class I pathway and a Pex19p- and Pex3p-independent class II pathway. We show here that Pex19p plays an essential role as the chaperone for full-length Pex3p in the cytosol. Pex19p forms a soluble complex with newly synthesized Pex3p in the cytosol and directly translocates it to peroxisomes. Knockdown of Pex19p inhibits peroxisomal targeting of newly synthesized full-length Pex3p and results in failure of the peroxisomal localization of Pex3p. Moreover, we demonstrate that Pex16p functions as the Pex3p-docking site and serves as the peroxisomal membrane receptor that is specific to the Pex3p–Pex19p complexes. Based on these novel findings, we suggest a model for the import of PMPs that provides new insights into the molecular mechanisms underlying the biogenesis of peroxisomes and its regulation involving Pex3p, Pex19p, and Pex16p.

Introduction

Of over a dozen subcellular compartments in eukaryotic cells, the peroxisome is a spherical single membrane–bounded organelle that functions in essential metabolic pathways, including the β oxidation of very long chain fatty acids and the biosynthesis of ether lipids such as plasmalogens (van den Bosch et al., 1992). Peroxisomal matrix and membrane proteins (PMPs) are synthesized on free polysomes in the cytosol and are post-translationally imported into peroxisomes (Lazarow and Fujiki, 1985). The import of matrix proteins involves the recognition of two distinct topogenic signals, tripeptide peroxisomal targeting signal type 1 and nonapeptide peroxisomal targeting signal type 2, by their respective cytosolic receptors, Pex5p and Pex7p, followed by the translocation of such complexes via peroxisomal membrane importomers, which include Pex14p and RING peroxins (Heiland and Erdmann, 2005; Miyata and Fujiki, 2005; Fujiki et al., 2006b). Genetic phenotype complementation assays of peroxisome membrane-deficient mutants of yeast and mammalian cells led to the isolation of Pex3p, Pex16p, and Pex19p, which are all indispensable for PMP import (Hoehfeld et al., 1991; Eitzen et al., 1997; Honsho et al., 1998; Goette et al., 1998; Matsuzono et al., 1999; South and Gould, 1999; Ghaedi et al., 2000; Muntau et al., 2000). In contrast to the matrix protein import, the molecular mechanisms underlying the assembly of PMPs remain poorly defined (Fujiki et al., 2006a; Platta and Erdmann, 2007).

Jones et al. (2004) recently proposed that at least two different pathways, termed class I and class II, mediate PMP import. The class I pathway depends on Pex19p, a predominantly cytosolic protein that binds to the internal regions of peroxisomal membrane-targeting signal (mPTS) in multiple PMPs and functions as a chaperone and/or soluble receptor for newly synthesized PMPs. Pex3p was shown to be a membrane import receptor for class I PMPs by means of *PEX3* RNAi (Fang et al., 2004). The class II pathway was postulated to be independent of Pex19p and Pex3p and includes Pex3p as the only PMP cargo yet identified. Mammalian Pex3p is a 42-kD peroxisomal integral membrane protein containing three hydrophobic regions, of which two domains residing at the N-terminal part are

Correspondence to Yukio Fujiki: yfujiscb@mbox.nc.kyushu-u.ac.jp

Abbreviations used in this paper: HA, influenza virus hemagglutinin; mPTS, peroxisomal membrane-targeting signal; PMP, peroxisomal membrane protein; PNS, postnuclear supernatant; SB, semi-intact cell buffer; TM, transmembrane.

The Rockefeller University Press $30.00
J. Cell Biol. Vol. 183 No. 7 1275–1286
www.jcb.org/cgi/doi/10.1083/jcb.200806062

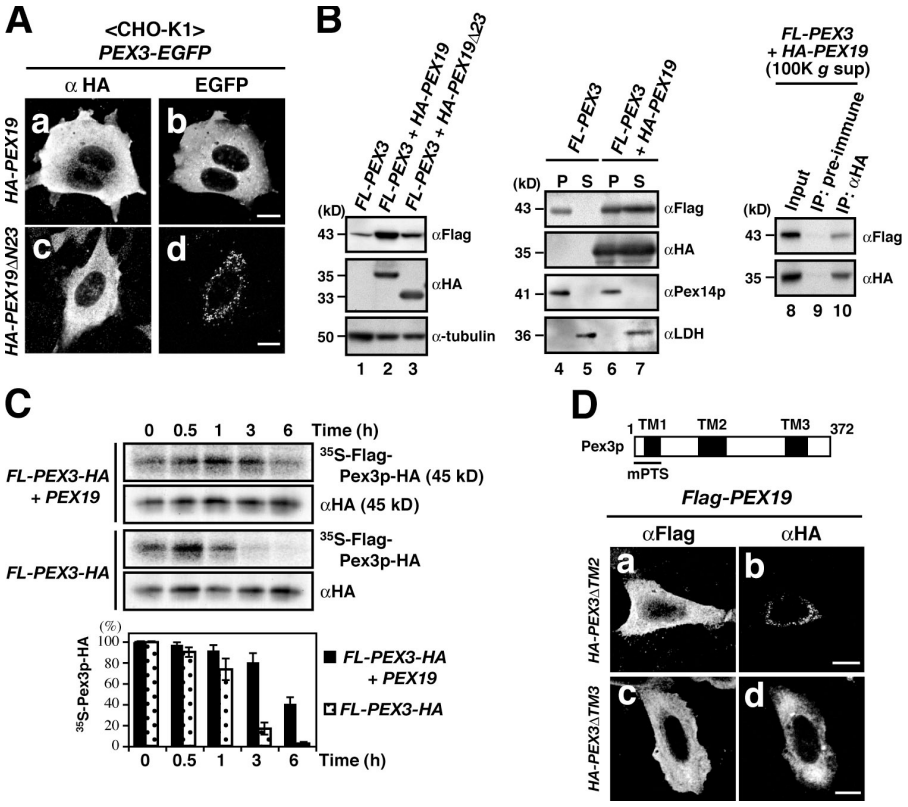

Figure 1. **Pex19p stabilizes Pex3p in the cytosol by forming Pex3p–Pex19p complexes.** (A) CHO-K1 cells were transfected with *PEX3-EGFP* together with *HA-PEX19* (a and b) or *HA-PEX19ΔN23* encoding HA-Pex19p truncated in amino acid residues 1–23 (c and d). After cell fixation, HA-Pex19p and Pex3p-EGFP were detected with anti-HA antibody (a and c) and by EGFP fluorescence (b and d), respectively. Bars, 10 μm. (B, left) CHO-K1 cells were transfected with *Flag-PEX3* plus a mock vector (lane 1), *HA-PEX19* (lane 2), or *HA-PEX19ΔN23* (lane 3). Cell lysates were analyzed by SDS-PAGE and immunoblot. α-Tubulin was used for a protein loading control. (middle) Organelle (P) and cytosol (S) fractions from PNS of CHO-K1 cells transfected with *Flag-PEX3* (lanes 4 and 5) or *Flag-PEX3* and *HA-PEX19* (lanes 6 and 7) were likewise analyzed. Separation of organelle and cytosol fractions were assessed with Pex14p and lactate dehydrogenase (LDH). Note that coexpression of Pex3p with Pex19p enhanced the level of Pex3p in the cytosol. (right) Immunoprecipitation of HA-Pex19p was performed with anti-HA antibody (lane 10) or preimmune serum (lane 9) from the cytosol fraction of CHO-K1 cells that had been cotransfected with *Flag-PEX3* and *HA-PEX19*. Immunoprecipitates were analyzed with antibodies to Flag and HA. (input) 10% of the cytosol used for immunoprecipitation. (C) CHO-K1 cells transfected with *Flag-PEX3-HA* together with *PEX19* (top) or a mock vector (middle) were pulse labeled for 20 min with [^{35}S]methionine and [^{35}S]cysteine and chased for the time indicated at the top. Immunoprecipitates using anti-HA antibody were analyzed by SDS-PAGE followed by autoradiography and immunoblot. Molecular mass of Flag-Pex3p-HA is 45 kD. ^{35}S-Flag-Pex3p-HA level at each time point, relative to Flag-Pex3p-HA assessed with anti-HA antibody, was quantitated and represented as a percentage of that at chase-starting time (bottom). Values are means ± SD of three experiments. (D) Pex19p-mediated stabilization of Pex3p in the cytosol requires the TM2-containing Pex19p-binding region. (top) A schematic view of rat Pex3p, where the potential TM3-encompassing residues at 311–332 are also indicated. (bottom) CHO-K1 cells were transfected with *Flag-PEX19* together with *HA-PEX3ΔTM2* or *HA-PEX3ΔTM3*. Cells were fixed and stained with antibodies to Flag (a and c) and HA (b and d). Bars, 10 μm.

reported as transmembrane 1 (TM1) and TM2 (Kammerer et al., 1998; Ghaedi et al., 2000; see also Fig. 1 D). Pex19p appears not to function as a chaperone and an import receptor for the Pex3p mPTS comprising the N-terminal first TM1 region. Instead, Pex19p binds to the TM2 part of Pex3p (Fang et al., 2004), implying that Pex19p may be required for preventing the aggregation of Pex3p-TM2. In contrast, in the yeast *Saccharomyces cerevisiae*, Pex3p (ScPex3p) fused to yellow fluorescent protein was constitutively transported to peroxisomes via the ER, where Pex19p was then required for the exit of Pex3p from the ER (Hoepfner et al., 2005). However, the precise role of ScPex19p in such processes has remained elusive.

In the present work, we first investigated whether Pex19p has a chaperone activity toward full-length Pex3p as for the class I PMPs. Our results show that Pex19p stabilizes newly synthesized full-length Pex3p in the cytosol and that this Pex3p–Pex19p complex is competent in the peroxisome-targeting assay using semi-intact CHO-K1 cells. Moreover, knockdown of endogenous Pex19p interferes with peroxisomal targeting of Pex3p. In vitro import assay, Pex3p is directly imported to peroxisomes in a Pex16p-dependent manner, whereas the knockdown of Pex16p significantly abrogates peroxisomal targeting of Pex3p. Based on these and earlier findings, we present a new model for membrane assembly of peroxisomes.

Results

Pex19p stabilizes Pex3p in the cytosol

Coexpression in CHO-K1 cells of full-length Pex3p fused to EGFP at the C terminus (Pex3p-EGFP) with N-terminally tandem influenza virus hemagglutinin (HA)–tagged Pex19p (HA-Pex19p; Matsuzono and Fujiki, 2006) gave rise to cytosolic localization of Pex3p-EGFP, whereas coexpression with HA-Pex19pΔN23 (Pex19p truncated in the N-terminal residues 1–23 and defective in binding to Pex3p [Matsuzono et al., 2006]) resulted in localization of Pex3p-EGFP to peroxisomes (Fig. 1 A). This was compatible with the findings that Pex3p interacted with the N-terminal part of Pex19p in the yeast and mammalian two-hybrid assays (Fransen et al., 2001; Fang et al., 2004). Compared with HA-Pex19pΔN23–expressing and mock cells, the expressed level of Flag-Pex3p was significantly elevated in HA-Pex19p–expressing cells (Fig. 1 B, lanes 1–3), where Flag-Pex3p was localized more in the cytosol in a form of Pex3p–Pex19p complexes (lanes 4–10). HA-Pex19p was likewise increased in the organelle fraction, more likely reflecting the HA-Pex19p binding to a higher level of Flag-Pex3p localized to peroxisomes (Fig. 1 B, lane 6; Matsuzono et al., 2006). Furthermore, to determine whether Pex19p stabilizes the full-length Pex3p, we performed a pulse-chase experiment. CHO-K1 cells

expressing Flag-Pex3p-HA, together with and without Pex19p, were pulse labeled for 20 min with [^{35}S]methionine and [^{35}S]cysteine, and then chased for 6 h. Flag-Pex3p-HA including ^{35}S-Flag-Pex3p-HA was immunoprecipitated, analyzed by immunoblot and autoradiography, and quantitated by a densitometer. ^{35}S-Flag-Pex3p-HA showed an apparent half-life of ~6 h when coexpressed with Pex19p, in contrast to ~2 h without Pex19p (Fig. 1 C), suggesting that Flag-Pex3p-HA was stabilized by Pex19p. Moreover, a Flag-Pex3p-HA mutant deleted in the TM2 domain, including Pex19p-docking region, failed to form the cytosolic complex with Pex19p, whereas another TM3-truncated variant was discernible in the cytosol as the Flag-Pex3p-HA (Fig. 1 D). These results strongly suggested that the TM2 domain was required for Pex19p-mediated stabilization of Pex3p. Collectively, it is most likely that Pex19p also functions as a chaperone for Pex3p as for the class I PMPs. Our conclusion was consistent with the observation that Pex3p and Pex14p bound to Pex19p in a competitive manner (Sacksteder et al., 2000).

Pex19p is involved in peroxisomal targeting of Pex3p

To verify whether Pex19p is responsible for peroxisomal targeting of newly synthesized Pex3p, we next investigated Pex3p translocation in cells where Pex19p was knocked down. In HEK293 cells transfected with control siRNA, both Pex3p-Myc and Pex3p(1–50)-Myc were colocalized with Pex14p, hence inciting proper translocation of Pex3p-Myc and Pex3p(1–50)-Myc to peroxisomes (Fig. 2 B, g–l). Pex19p was brilliantly discernible as numerous punctate structures colocalized with Pex14p (peroxisomes) compared with relatively weak and diffused staining of the cytosol (Fig. 2 B, h and k). Subcellular fractionation of HEK293 cell homogenates indicated that Pex19p distributed nearly equally between the organelle and cytosol fractions (unpublished data), thereby confirming the morphological observation. In contrast, in Pex19p knockdown cells (Fig. 2 A), Pex3p-Myc was discernible predominantly in other organelles apparently including mitochondria, whereas Pex3p(1–50)-Myc was correctly imported into peroxisomes (Fig. 2 B, a–f). Furthermore, we assessed Pex3p-Myc and Pex3p(1–50)-Myc import-competent cells in several hundreds of cells where Pex19p was knocked down as well as in randomly selected cells transfected with a control siRNA. Statistic analysis of these data confirmed that the elimination of Pex19p gave rise to the specific defect in the import to peroxisomes of full-length Pex3p, but not Pex3p(1–50)-Myc (Fig. 2 C). Collectively, these results demonstrated that Pex19p was essential for peroxisomal targeting of newly synthesized full-length Pex3p in vivo.

Pex16p functions as a membrane receptor for Pex3p–Pex19p complexes

To investigate whether Pex3p–Pex19p complexes in the cytosol are competent to translocate to peroxisomes, we performed PMP-targeting assay at 26°C for 1 h using the semi-intact CHO-K1 cells that had been permeabilized with digitonin. After incubation of the semi-intact cells with the cytosol fraction containing Pex3p-Myc and HA-Pex19p, both proteins were detected in a

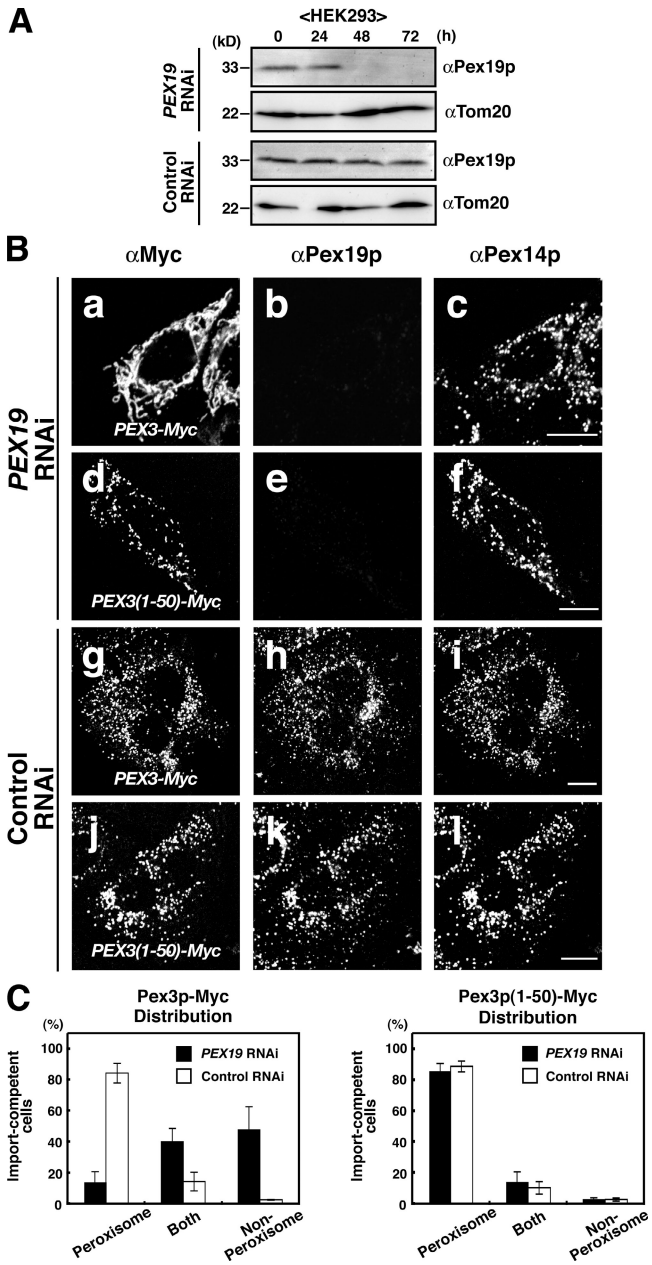

Figure 2. **The effect of Pex19p on the localization of Pex3p.** (A) HEK293 cells were transfected with *PEX19* RNAi or control RNAi twice at a 24-h interval (the first siRNA treatment is day 0). Cells were lysed each day after the siRNA treatment, and equivalent volumes of total cell lysates were analyzed by SDS-PAGE and immunoblot. Tom20 was used for a protein loading control. (B) Depletion of Pex19p abrogates Pex3p targeting in vivo. On day 2 after siRNA treatment, *PEX19* RNAi (a–f)- or control RNAi (g–l)-transfected cells were retransfected with *PEX3-Myc* (a–c and g–i) or *PEX3(1–50)-Myc* (d–f and j–l). Pex3p-Myc, Pex3p(1–50)-Myc, Pex19p, and Pex14p were detected by cell staining using antibodies to Myc (a, d, g and j), Pex19p (b, e, h and k), and Pex14p (c, f, i and l), respectively. Bars, 10 μm. Note that in HEK293 cells, endogenous Pex19p was detected as particles, colocalized with the peroxisomal marker Pex14p. (C) Control siRNA-transfected or -mediated Pex19p knockdown cells were assessed for the level and subcellular localization of Pex3p-Myc and Pex3p(1–50)-Myc by immunostaining. (left) Cell phenotypes with respect to the localization of Pex3p-Myc were classified into three types, peroxisomal, nonperoxisomal, and both, and was represented as a percentage of total cells counted. Values are means ± SD of three experiments. Control siRNA, n = 462; *PEX19* siRNA, n = 454. (right) Localization of Pex3p(1–50)-Myc was likewise verified. Control siRNA, n = 542; *PEX19* siRNA, n = 416.

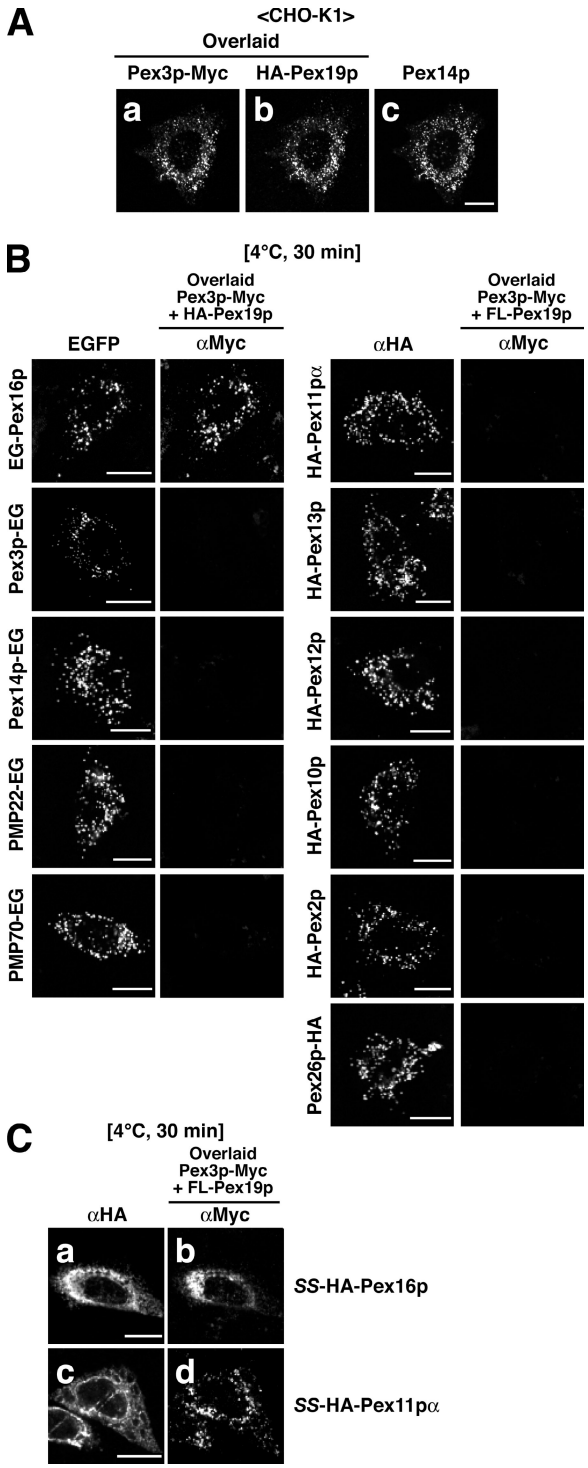

Figure 3. **Pex16p functions as a membrane receptor for Pex3p–Pex19p complexes.** (A) Pex3p-targeting assay was performed at 26°C for 1 h using semipermeabilized CHO-K1 cells and cytosol fraction containing Pex3p-Myc and HA-Pex19p, as described in Materials and methods. Pex3p-Myc, HA-Pex19p, and Pex14p were detected with antibodies to Myc (a), HA (b), and Pex14p (c), respectively. Bar, 10 µm. (B) Pex3p-targeting assay using the semipermeabilized cells was done at 4°C for 30 min. (left) Semipermeabilized cells used were CHO-K1 cells expressing EGFP-fused membrane peroxins (Pex-EGs) and PMPs (PMP-EGs). The assays were performed with cytosol fraction containing Pex3p-Myc and HA-Pex19p. Membrane peroxins and Pex3p-Myc were visualized by GFP fluorescence and staining with anti-Myc antibody, respectively. (right) Semi-intact CHO-K1 cells expressing HA-tagged membrane peroxins were likewise verified with cytosol fraction containing Pex3p-Myc and Flag-Pex19p. HA peroxins were detected with anti-HA antibody. All EGFP-fused or HA-tagged membrane peroxins used are biologically active in CHO mutants and human fibroblasts derived from patients with peroxisome biogenesis disorders (not depicted). Bars, 10 µm. Note that ectopic expression of EGFP-Pex16p specifically enhanced the targeting efficiency of Pex3p-Myc. (C) ER-localized Pex16p recruits Pex3p–Pex19p complexes to ER membranes. *SS-HA-PEX16* and *SS-HA-PEX11a* encoding HA-Pex16p and HA-Pex11pα, both N-terminally tagged with the signal sequence of mouse activin type IIA receptor, were expressed in CHO-K1 cells. Cells were semipermeabilized and assayed for Pex3p-Myc targeting as in B. HA-Pex16p (a), Pex3p-Myc (b and d), and HA-Pex11pα (c) were detected by immunostaining. Bars, 10 µm.

manner superimposable on Pex14p (Fig. 3 A and Fig. S1 A, available at http://www.jcb.org/cgi/content/full/jcb.200806062/DC1), thereby indicating that Pex3p–Pex19p complexes and possibly Pex19p were transported to peroxisomes. As a control, when only Pex3p-Myc was expressed by transient transfection of *PEX3-Myc* to CHO-K1 cells, Pex3p-Myc was not found in the cytosol fraction, but was partly aggregated or mislocalized to mitochondria (unpublished data), as reported previously (Sacksteder et al., 2000; Matsuzono et al., 2006). Transiently expressed HA-Pex19p was mostly in the cytosol and competent in targeting to peroxisomes, at endogenous or ectopically expressed Pex3p level in the targeting assay using semi-intact cells (unpublished data). Next, we search for a potential membrane receptor for Pex3p–Pex19p complexes, using the semi-intact cells that had been ectopically and transiently expressed with EGFP-fused or HA-tagged PMPs including membrane-integrated peroxins. To more readily and specifically detect the targeting of Pex3p-Myc to ectopically expressed PMPs on peroxisomes, the targeting assay was performed at 4°C for 30 min, under which condition, using mock-transfected CHO-K1 cells, the targeting of Pex3p-Myc and HA-Pex19p complex to "naive" peroxisomes was relatively less discernible (unpublished data). Upon incubation at 4°C for 30 min, peroxisomal localization of Pex3p-Myc was enhanced only in the cells expressing EGFP-Pex16p in a superimposable manner (Fig. 3 B and Fig. S1 B), with five- to sixfold increase in the level of targeted Pex3p-Myc as compared with the control cells where Pex3p-Myc was barely discernible (Fig. S2, available at http://www.jcb.org/cgi/content/full/jcb.200806062/DC1), thereby suggesting that Pex16p is a receptor for Pex3p–Pex19p complexes. It was noteworthy that the Pex3p-Myc targeted to peroxisomes at 4°C was barely integrated to membranes as assessed by the sodium carbonate extraction (Fujiki et al., 1982; unpublished data). In the similar assay using CHO-K1 cells stably expressing Pex16p-HA (unpublished data; Honsho, M.), after 1-h targeting incubation at 0°C, Pex3p-Myc became resistant to the alkaline extraction upon a chase reaction for 1 h at 26°C, but not 0°C, with no difference between the presence of ATP plus ATP-regenerating system and AMP-PNP (Fig. S3), thereby indicating the integration of Pex3p-Myc to peroxisome membranes in a manner dependent on temperature but independent of ATP hydrolysis.

In our attempts to detect and/or isolate the endogenous Pex3p–Pex19p complexes in the cytosol, it was very difficult to detect them because of the extremely low level of such transient complexes, in not only wild-type CHO-K1 cells but also *pex16* mutant fibroblasts from the *PEX16*-defective patient with Zellweger

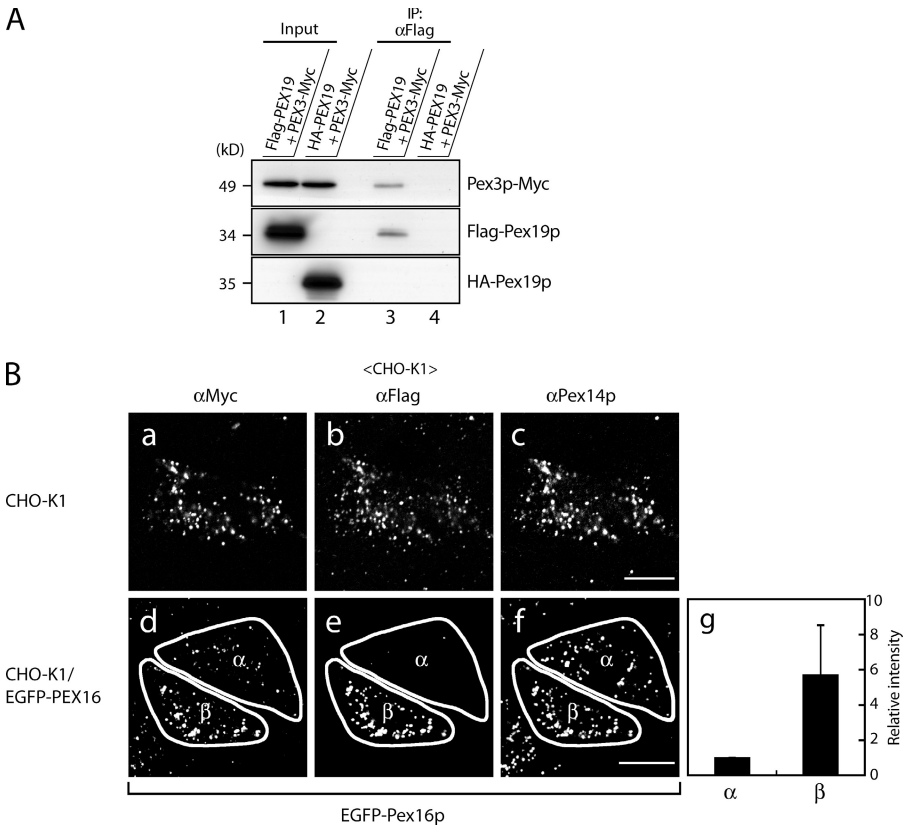

Figure 4. **Pex3p–Pex19p complexes formed in the cytosol are competent to translocate to peroxisomes in a Pex16p-dependent manner.** (A) Purification of cytosolic Pex3p–Pex19p complexes. Immunoprecipitation was performed with anti-Flag IgG-conjugated agarose (Sigma-Aldrich) from the cytosol fractions of CHO-K1 cells that had been transfected with *PEX3-Myc* together with *Flag-PEX19* (lanes 1 and 3) or *HA-PEX19* as a control (lanes 2 and 4). Immunoprecipitates were eluted with Flag peptide and subjected to SDS-PAGE and immunoblotting using antibodies to Myc, Flag, and HA. Note that Pex3p-Myc was specifically immunoprecipitated and coeluted with Flag-Pex19p (lane 3). (B) Cytosolic Pex3p-Myc–Flag-Pex19p complexes are imported to peroxisomes in a Pex16p-dependent manner. In vitro targeting assay was performed at 26°C for 1 h using semipermeabilized CHO-K1 cells (a–c) and *EGFP-PEX16*-transfected CHO-K1 cells (d–f) with the eluted fraction in A (lane 3) containing Pex3p-Myc–Flag-Pex19p complexes. Before the targeting assay, Flag peptide was removed from the eluted fraction by gel filtration chromatography on a Sephadex G-25. Pex3p-Myc, Flag-Pex19p, and Pex14p were detected with antibodies to Myc (a and d), Flag (b), and Pex14p (c and f), respectively. EGFP-Pex16p was detected by EGFP fluorescence (e). Bars, 10 μm. (g) Pex3p-Myc levels in cells expressing EGFP-Pex16p at higher (β) and nearly basal (α) levels were quantitated by calculating the ratio of the integrated fluorescence intensities of Pex3p-Myc to Pex14p using LSM software and shown by taking 1 as the value in the cell (α). Values are means ± SD (n = 6).

syndrome where Pex3p was readily mistargeted to other organelles such as mitochondria (unpublished data).

To assess if Pex16p is sufficient as the membrane receptor for Pex3p–Pex19p complexes, we expressed in ER membranes of CHO-K1 a HA-Pex16p variant of which the N terminus was fused with the signal sequence of mouse activin type IIA receptor (Matsuzaki et al., 2002) termed SS-HAPex16p. In the semipermeabilized cells expressing SS-HA-Pex16p, Pex3p-Myc coincided in the localization with SS-HA-Pex16p, not with SS-HA-Pex11pα chosen as a control; hence indicating specific targeting of Pex3p to the ER-localized Pex16p (Fig. 3 C). We interpreted this finding to mean that Pex16p was sufficient for recruiting Pex3p–Pex19p complexes to peroxisome membranes. Moreover, both N- and C-terminal regions of Pex16p were indispensable for recruiting the Pex3p–Pex19p complexes to peroxisomes as likewise assayed using the semi-intact cell import system (Fig. S4, available at http://www.jcb.org/cgi/content/full/jcb.200806062/DC1).

Pex16p functions as a membrane receptor for cytosolic Pex3p–Pex19p complexes

To confirm that Pex3p–Pex19p complexes formed in the cytosol are translocated to peroxisomes, we performed in vitro targeting assay using immunoaffinity-purified Pex3p–Pex19p complexes. From the cytosol fractions from CHO-K1 cells that had been transfected with *PEX3-Myc* and either *Flag-PEX19* or *HA-PEX19*, immunoprecipitation was performed with Flag-agarose. Immunoprecipitates were eluted with Flag peptide. Pex3p-Myc was specifically eluted with Flag-Pex19p (Fig. 4 A), indicating that Pex3p-Myc formed a complex with Flag-Pex19p. After incubation of the semi-intact cells with the eluted fraction containing Pex3p-Myc–Flag-Pex19p complexes, both proteins were detected in a manner superimposable on Pex14p (Fig. 4 B, a–c), thereby indicating that Pex3p-Myc–Flag-Pex19p complexes were indeed transported to peroxisomes. Furthermore, we demonstrated that peroxisomal import of Pex3p-Myc–Flag-Pex19p complexes was enhanced in the cells expressing EGFP-Pex16p, with five- to sixfold increase in the level of targeted Pex3p-Myc as compared with the control cells (Fig. 4 B, d–g), thereby indicating that Pex16p functions as a receptor for cytosolic Pex3p–Pex19p complexes.

Pex16p-mediated Pex3p import to peroxisomes in the absence of ER

Next, we investigated whether Pex3p is directly imported into peroxisomes in the absence of ER membranes. We performed in vitro Pex3p import assay at 26°C for 1 h using cell-free synthesized Pex3p-Myc and highly purified peroxisomes from CHO-K1 as well as those from CHO-K1 cells stably expressing HA-Pex16p (Fig. 5 A). Pex3p-Myc was detected only in peroxisomes not in mitochondrial and rough and smooth microsomal fractions, and the Pex3p-Myc level was elevated severalfold with peroxisomes harboring the ectopically expressed HA-Pex16p (Fig. 5 B). The Pex3p-Myc in peroxisomes was resistant to the alkaline extraction (Fujiki et al., 1982), hence indicating that Pex3p was

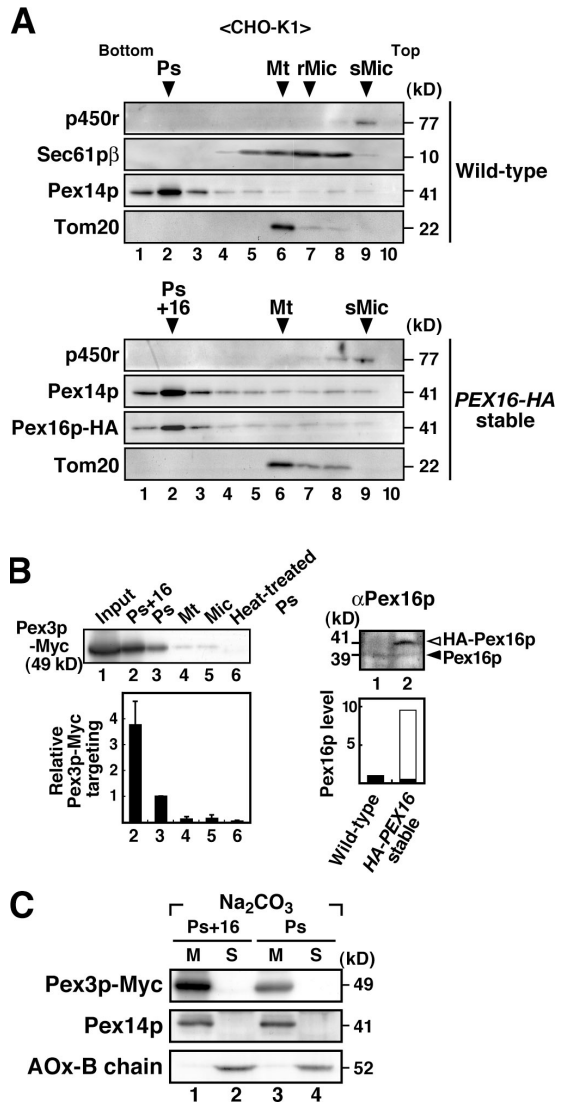

Figure 5. **Pex3p is directly imported into peroxisomes.** (A) Subcellular fractionation of wild-type CHO-K1 cells and those stably expressing Pex16p-HA. Organelle fractions from respective PNS fractions were separated by OptiPrep density gradient ultracentrifugation as described in Materials and methods. Distribution of peroxisomes, mitochondria, and ER (smooth and rough microsomes) were verified by immunoblotting using antibodies against marker proteins: Pex14p, Tom20, P450 reductase, and Sec61pβ, respectively. Arrowheads and bars indicate the peak fractions of peroxisomes (Ps; lane. 2, top), mitochondria (Mt; lane 6, top), smooth and rough microsomes (sMic and rMic; lanes 9 and 6–8, respectively, top), and peroxisomes harboring Pex16p-HA (Ps+16; lane 2, bottom) that were used for in vitro import assays in B. (B) Pex3p-Myc is directly translocated to peroxisomes in a Pex16p-dependent manner. (left) In vitro Pex3p-Myc import assays were performed using Pex3p-Myc synthesized together with Pex19p in a rabbit reticulocyte-lysate system. Pex3p-Myc was incubated at 26°C for 1 h with equal protein amounts of peroxisomes (lane 3), mitochondria plus rough microsomes (lane 4), smooth microsomes (lane 5), and peroxisomes harboring Pex16p-HA (lane 2), respectively, in SB. The same amount of peroxisome fraction was heat denatured and used as an import-negative control (lane 6). After the reaction, organelles were recovered by centrifugation and analyzed by SDS-PAGE and immunoblot. Targeted Pex3p-Myc levels in each fraction were quantitated using ImageJ software and shown by taking 1 as the value in the peroxisome (lane 3) fraction (bottom). (right) Pex16p expression levels in wild-type and HA-Pex16p–expressing cells were assessed by SDS-PAGE and immunoblotting with anti-Pex16p antibody of equal protein amounts of organelle fractions. Closed and open arrowheads indicate endogenous Pex16p and Pex16p-HA, respectively. Total Pex16p levels were quantitated as in the left panel and shown by taking 1 as the value in the wild-type cells, in which the values are means ± SD of three experiments (bottom). Closed and open bars indicate the relative expression levels of endogenous Pex16p and Pex16p-HA, respectively. (C) Pex3p-Myc is targeted and integrated into peroxisomal membranes. After the in vitro import assays, peroxisome and peroxisomes harboring Pex16p-HA fractions (B, left) were treated with 0.1 M Na_2CO_3. Membrane (M) and soluble (S) fractions were analyzed by SDS-PAGE and immunoblotting using antibodies to Myc, Pex14p, and a matrix enzyme, acyl-CoA oxidase (AOx). Only AOx-B chain was shown.

integrated into peroxisome membranes (Fig. 5 C). These results strongly suggested that Pex3p was directly imported into peroxisomes via Pex3p receptor Pex16p on peroxisomal membranes.

Mechanism of Pex3p targeting mediated by Pex19p and Pex16p

To assess the functional role, if any, of Pex3p mPTS distinct from Pex19p-binding region in the targeting of Pex3p–Pex19p complex to Pex16p, we likewise performed the transport reaction using the semi-intact cells expressing EGFP-Pex16p with cytosolic fraction containing HA-Pex19p and Pex3p-Myc or mPTS-deleted Pex3pΔN30-Myc. Pex3p-Myc was efficiently translocated to EGFP-Pex16p-positive particles (peroxisomes), whereas Pex3pΔN30-Myc apparently failed to target EGFP-Pex16p (Fig. 6, A and B). These data strongly suggested that Pex3p mPTS was essential for the Pex3p–Pex19p complex to translocate and bind to Pex16p on peroxisome membranes. Next, we attempted to delineate the roles of Pex16p and Pex19p in membrane targeting of Pex3p, using the full-length Pex3p-Myc and mPTS-containing Pex3p(1–50)-Myc that had been synthesized as such or together with HA-Pex19p in a cell-free translation system. In the Pex3p transport assays using semi-intact cells, ectopic expression of EGFP-Pex16p significantly enhanced the peroxisomal targeting of not only Pex3p-Myc but also Pex3p(1–50)-Myc (Fig. 6 C, a, c, i, and k). The Pex3p-Myc translocation to peroxisomes was specifically enhanced by its co-translation with HA-Pex19p in both control and EGFP-Pex16p–expressing cells (Fig. 6 C, a, b, i, and j). However, no such apparent effect of HA-Pex19p was discernible on Pex3p(1–50)-Myc in both types of cells (Fig. 6 C, c, d, k, and l). Statistical analysis of these data confirmed the Pex16p- and Pex19p-dependent enhancement of the specific targeting of Pex3p-Myc as well as Pex16p-dependent but Pex19p-independent increase in translocation of Pex3p(1–50)-Myc (Fig. 6 D). Moreover, cell-free synthesized Pex3p-Myc and Pex3p(1–50)-Myc, but not Pex3pΔN30-Myc, were coimmunoprecipitated with Flag-Pex16p-HA, thereby indicating the direct binding of Pex3p as well as Pex3p(1–50) to Pex16p (Fig. 7, A and B). However, ectopically expressed Pex16p on peroxisome membranes did not recruit the cytosolic Pex19p in semi-intact cells (unpublished data). Collectively, it is most likely that Pex19p simply prevents Pex3p from mistargeting by its chaperoning activity and promotes Pex16p-dependent Pex3p targeting via interaction of the Pex3p mPTS with Pex16p.

Pex16p is the membrane receptor for Pex3p in vivo

To verify whether Pex16p functions as a membrane receptor for newly synthesized Pex3p in vivo, we first investigated Pex3p

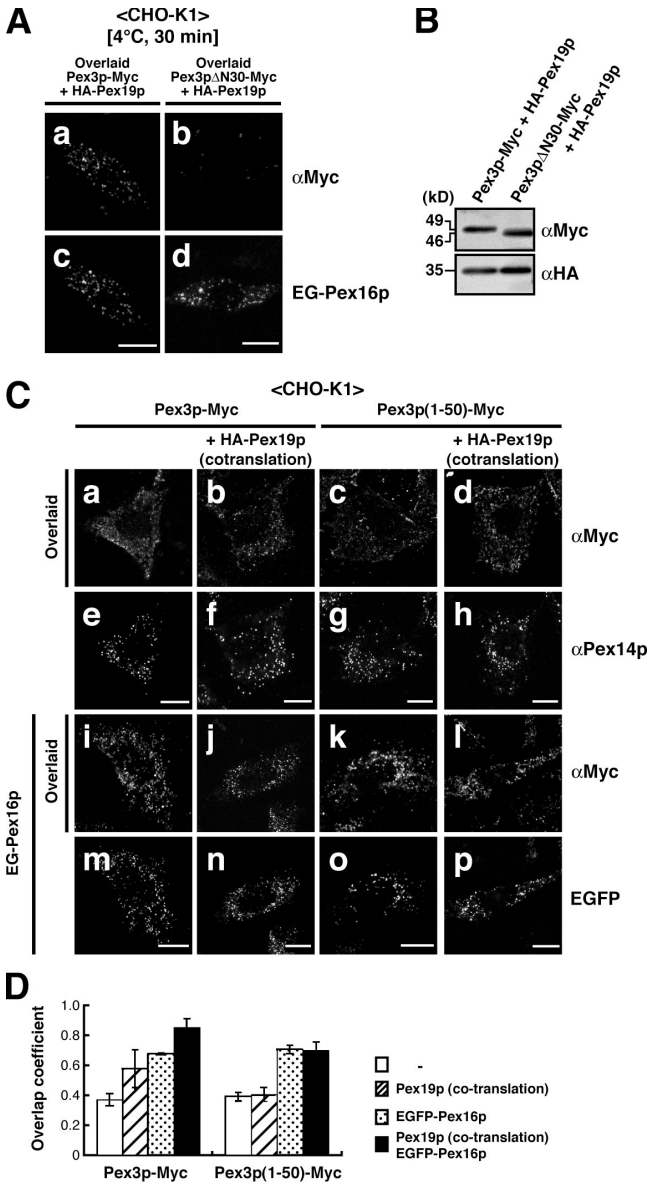

Figure 6. **N-terminal domain of Pex3p is essential for translocation to peroxisome membranes.** (A) N-terminal mPTS region of Pex3p is involved in docking to Pex16p. Pex3p import assay in semi-intact CHO-K1 was performed as in Fig. 3 B, with the cytosol fraction containing HA-Pex19p and Pex3p-Myc (left) or Pex3pΔN30-Myc truncated in 30 residues from the N terminus (right). EGFP-Pex16p and Myc-tagged Pex3p and Pex3pΔN30 were detected by GFP fluorescence and immunostaining with anti-Myc antibody. Bars, 10 μm. (B) Cytosol fractions used in A were verified by SDS-PAGE and immunoblotting. (C) N-terminal domain of Pex3p targets peroxisomes in a Pex16p-dependent but Pex19p-independent manner. Pex3p-Myc and Pex3p(1–50)-Myc were synthesized by cell-free translation (a, c, i, and k) or cotranslation with HA-Pex19p (b, d, j, and l) in a rabbit reticulocyte-lysate system. Supernatant fractions were incubated at 26°C for 1 h with semipermeabilized, CHO-K1 cells (a–h) and *EGFP-PEX16*–transfected CHO-K1 cells (i–p). Cells were stained with antibodies to Myc and Pex14p. EGFP-Pex16p (m–p) was detected by GFP fluorescence. Bars, 10 μm. (D) Peroxisome-targeting specificities of Pex3p-Myc and Pex3p(1–50)-Myc were determined by quantitative analysis of confocal images in C. Manders overlap coefficient (Manders et al., 1993) between peroxisomes (marked by Pex14p or EGFP-Pex16p) and Pex3p-Myc or Pex3p(1–50)-Myc were calculated with ImageJ software. Values are means ± SD of at least three experiments. Pex3p-Myc: open bar, $n = 4$; diagonal bar, $n = 3$; dotted bar, $n = 3$; solid bar, $n = 6$. Pex3p(1–50)-Myc: all bars, $n = 3$. Note that peroxisome-targeting specificity of Pex3p(1–50)-Myc was dependent on Pex16p but not Pex19p.

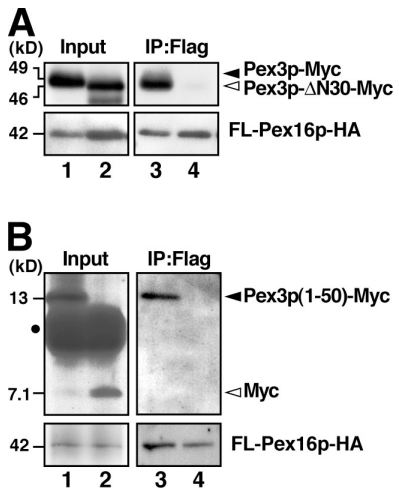

Figure 7. **mPTS of Pex3p binds to Pex16p.** (A) Pex3p-Myc and Pex3pΔN30-Myc were synthesized in vitro by cotranslation with Flag-Pex16p-HA mRNA. The reaction mixture was centrifuged and the supernatant was subjected to immunoprecipitation (IP) with anti-Flag IgG agarose. Bound proteins were eluted with Flag peptides and analyzed by SDS-PAGE and immunoblotting with antibodies to Myc and HA. Lanes 1 and 2, 10% input of Pex3p-Myc and Pex3pΔN30-Myc; lanes 3 and 4, immunoprecipitates. (B) Flag-Pex16p-HA was likewise synthesized by cell-free translation with Pex3p(1–50)-Myc or Myc. Immunoprecipitation was done as in A. Lanes 1 and 2, 10% input of Pex3p(1–50)-Myc or Myc; lanes 3 and 4, immunoprecipitates. Dot indicates endogenous globin apparently cross reacting with anti-Myc antibody.

targeting in cells ectopically expressing Pex16p. CHO-K1 cells were transfected with *PEX3-Myc* or *Myc-PEX12* together with *PEX16(Δ66-81)-HA* coding for a Pex16p-HA mutant lacking the amino acid sequence 66–81 containing the mPTS (Honsho et al., 2002). Pex16p(Δ66-81)-HA was localized to ER-like structures (Fig. 8 A, b), which is consistent with our earlier finding (Honsho et al., 2002). Pex3p-Myc mostly coincided with Pex16p(Δ66-81)-HA, indicative of its translocation to such structures, even in the presence of peroxisomes (Fig. 8 A, a–c), whereas Myc-Pex12p was localized to peroxisomes as assessed by staining of Pex14p (d–f). Pex3p(1–50)-Myc was likewise targeted to Pex16p(Δ66-81)-HA–positive membranes (Fig. 8 A, g–i). We interpreted these results to mean that Pex16p recruits newly synthesized Pex3p to Pex16p-residing membranes in vivo, in a Pex3p mPTS-dependent manner.

To confirm the Pex16p-dependent peroxisomal targeting of newly synthesized Pex3p, we investigated Pex3p translocation in cells where Pex16p was knocked down. HEK293 cells were transfected with siRNAs each for Pex16p, Pex13p, and a control EGFP. At 40 h after the transfection, cells were transfected with plasmids each encoding Pex3p-Myc and HA-Pex11pα and were cultured for 12 h, fixed, and stained with specific antibodies. In cells transfected with control siRNA, Pex3p-Myc was colocalized with Pex14p, Pex16p, and Pex13p, hence indicating proper translocation of Pex3p-Myc to peroxisomes (Fig. 8 B, a–f). Pex3p-Myc was likewise transported to peroxisomes in Pex13p knockdown cells (Fig. 8 B, g–i). In contrast, in Pex16p knockdown cells, Pex3p-Myc was discernible predominantly in other organelles possibly including mitochondria (Fig. 8 B, j–l), whereas HA-Pex11pα was correctly targeted to peroxisomes (m–o). However, Pex3p-Myc import was not

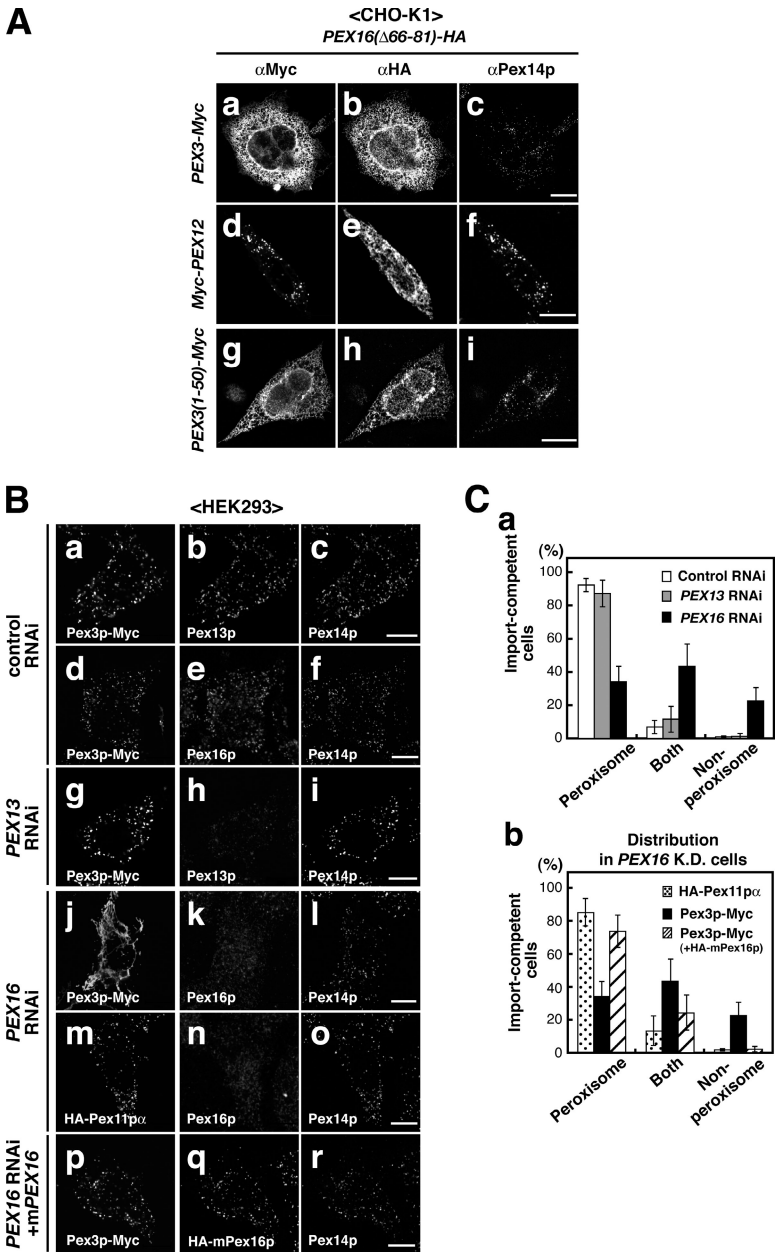

Figure 8. **Pex16p is the membrane receptor for Pex3p.** (A) Mislocalization of Pex16p induces mistargeting of coexpressed Pex3p in vivo. CHO-K1 cells were transfected with *PEX16(Δ66-81)-HA* together with *PEX3-Myc* (a–c), *Myc-PEX12* (d–f), or *PEX3(1–50)-Myc* (g–i). Cells were fixed and stained with antibodies to Myc (a, d, and g), HA (b, e, and h), and Pex14p (c, f, and i). Bars: (a–c and g–i) 20 μm; (d–f) 10 μm. (B) Depletion of Pex16p abrogates Pex3p targeting in vivo. HEK293 cells were transfected with siRNAs each for a control EGFP (a–f), *PEX13* (g–i), and *PEX16* (j–r). After 40 h, cells were transfected with *PEX3-Myc* (a–l), *HA-PEX11α* (m–o), and *PEX3-Myc* plus *HA-mPEX16*, a mutant *PEX16* with a silent mutation in the target sequence of *PEX16* siRNA (p–r). Pex3p-Myc, HA-Pex11pα, HA-mPex16p, Pex13p, Pex16p, and Pex14p were detected by cell staining using antibodies to Myc (a, d, g, j, and p), HA (m and q), Pex13p (b and h), Pex16p (e, k, and n), and Pex14p (c, f, i, l, o, and r), respectively. Bars, 10 μm. (C, a) Control siRNA-transfected or -mediated Pex16p or Pex13p knockdown cells were assessed for the level and subcellular localization of Pex3p-Myc by immunostaining. Cell phenotypes with respect to the localization of Pex3p-Myc were classified into three types, peroxisomal, nonperoxisomal, and both, and were represented as percentages of total cells counted. Values are means ± SD of three experiments. Control EGFP siRNA, $n = 521$; *PEX13* siRNA, $n = 515$; *PEX16* siRNAi, $n = 519$. (b) siRNA-mediated Pex16p knockdown cells were likewise verified for subcellular location of HA-Pex11pα, Pex3p-Myc, and Pex3p-Myc coexpressed with HA-mPex16p. HA-Pex11pα, $n = 508$; Pex3p-Myc, $n = 519$; Pex3p-Myc with HA-mPex16p, $n = 651$.

affected when *PEX16* siRNA was cotransfected with mutant *PEX16* siRNA containing a silence mutation in the sequence for Pex16p mPTS (Fig. 8 B, p–r). In these cells, Pex16p was detectable at a normal level (Fig. 8 B, q). Furthermore, we assessed Pex3p import-competent cells in several hundred cells where Pex16p or Pex13p was knocked down as well as in randomly selected cells transfected with a control siRNA. Statistic analysis of these data confirmed that the severe reduction of Pex16p gave rise to the specific defect in Pex3p import to peroxisomes (Fig. 8 C). Collectively, these results demonstrated that Pex16p was a prerequisite for peroxisomal targeting of newly synthesized Pex3p in vivo, functioning as the Pex3p membrane receptor.

Discussion

Recent work (Fang et al., 2004; Jones et al., 2004) has proposed two mechanistically distinct pathways for the peroxisomal import of PMPs: the Pex3p- and Pex19p-dependent class I pathway and the Pex3p- and Pex19p-independent class II pathway. Categorization of the class II import pathway was largely based on the observation that Pex19p did not function as a chaperone and an import receptor for the mPTS of Pex3p. However, this work paid little attention to full-length Pex3p.

In the present work, we have shown that Pex19p plays an essential role as the chaperone for full-length Pex3p, as it also does for other class I PMPs. Knockdown of Pex19p inhibits peroxisomal targeting of newly synthesized full-length Pex3p (Fig. 2). In addition to the stabilization of Pex3p by Pex19p in the cytosol, the cytosolic Pex3p–Pex19p complexes are competent to translocate to peroxisomes (Figs. 3 and 4). Moreover, we have demonstrated from the following that Pex16p functions as the Pex3p-docking site: (a) the higher level expression of Pex16p, but not other PMPs, significantly enhances the efficiency in

peroxisomal targeting of not only Pex3p–Pex19p complexes in the cytosol but also the isolated cytosolic Pex3p–Pex19p complexes (Fig. 3 B, Fig. 4 B, Fig. S1, and Fig. S2) and cell-free synthesized Pex3p–Pex19p complexes (Fig. 5; and Fig. 6, C and D); (b) an ectopically expressed Pex16p variant lacking its mPTS recruits the Pex3p–Pex19p complexes to the membranes, such as ER harboring the Pex16p mutant (Fig. 3 C); (c) Pex16p directly interacts with Pex3p (Fig. 7); and (d) the siRNA-based knockdown of Pex16p abrogates peroxisomal targeting of newly synthesized Pex3p (Fig. 8 B). Taking these results together, we conclude that Pex16p plays both a necessary and a sufficient role in the selective targeting of Pex3p–Pex19p complexes.

We therefore propose a new classification of the pathways for the peroxisomal import of PMPs that depends on Pex19p-mediated membrane docking: (a) a class I pathway in which Pex3p functions as the membrane receptor, and (b) a class II pathway where Pex16p is the anchoring site. Under this new classification, the original class II pathway (Fang et al., 2004; Jones et al., 2004) for Pex3p–Pex19p–independent PMP import would (if its existence is confirmed) be included as an additional class III pathway.

Pex16p is known to be a class I PMP that is imported to peroxisomes by the Pex19p-dependent and Pex3p-mediated pathway (Fang et al., 2004; Jones et al., 2004; Matsuzono and Fujiki, 2006; Matsuzono et al., 2006). However, our study shows that Pex16p also functions as the membrane receptor for Pex3p. This raises an intriguing "chicken-and-egg" issue regarding the molecular events at the initial stages of peroxisome membrane biogenesis. Although we cannot yet provide a definitive resolution to this issue, we propose a consolidating model termed "mutual-dependent targeting," which both reconciles our findings and provides new mechanistic insights into peroxisome membrane biogenesis (Fig. 9). In this model, two types of membrane structures, initially harboring either Pex3p or Pex16p, are equally capable of developing into peroxisomes, implying that de novo membrane biogenesis may be initiated via two mutually distinct pathways. Peroxisome membranes are likely formed via these pathways, either independently or in a coordinated manner.

More recently, Pex16p was reported to function as a Pex3p receptor on ER membranes and to initiate de novo peroxisome membrane biogenesis from ER membranes (Kim et al., 2006). However, such a functional role of Pex16p on ER membranes was deduced from the results obtained by an overexpression system. It still remains unclear how Pex16p is imported into ER membranes and whether Pex16p serves as a Pex3p receptor only on ER membranes. In the present study, we demonstrated that Pex3p was directly imported into peroxisomes and that Pex16p functioned as the Pex3p receptor on peroxisomal membranes (Fig. 5). We also confirmed these findings with the semi-intact cell system (unpublished data). Given that Pex3p functions as a peroxisomal import receptor for multiple class I PMPs, the directly providing step of Pex3p via Pex16p to the preexisting peroxisomes may be a prerequisite for the maintenance of the sufficient import of various class I PMPs.

With respect to Pex16p in other species, the yeast *Yarrowia lipolytica* Pex16p (YlPex16p; Eitzen et al., 1997) shares 24% amino acid identity with the human Pex16p (Honsho et al., 1998). Despite the fact that intraperoxisomal peripheral membrane peroxin (YlPex16p) and an integral membrane protein (HsPex16p) are essential for peroxisome biogenesis, their roles do not appear to be identical (Eitzen et al., 1997; Titorenko et al., 1997; Honsho et al., 1998; Titorenko and Rachubinski, 1998; South and Gould, 1999; South et al., 2000). YlPex16p unlikely plays a role as the membrane receptor for YlPex3p. Furthermore, in *S. cerevisiae*, a *PEX16* homologue is not identified in the genome (South and Gould, 1999; Hettema et al., 2000), where the ScPex3p- and ScPex19p-dependent class I PMP import pathway is conserved (Fang et al., 2004). These observations imply that Pex16p-mediated regulation of Pex3p import is not conserved between yeast and mammalian cells and suggest the possibility that such a function of Pex16p may have evolved later in mammalian cells (Schlueter et al., 2006). The functional roles of mammalian Pex16p may be fulfilled by other peroxins, if any, in *Y. lipolytica* and *S. cerevisiae*. It is also equally possible that there may be other mechanisms underlying the Pex3p import in these species, as suggested previously (Hoepfner et al., 2005; Kragt et al., 2005; Tam et al., 2005). Addressing such issues would provide a comprehensive understanding of the molecular mechanisms that govern peroxisome membrane biogenesis in eukaryotic cells.

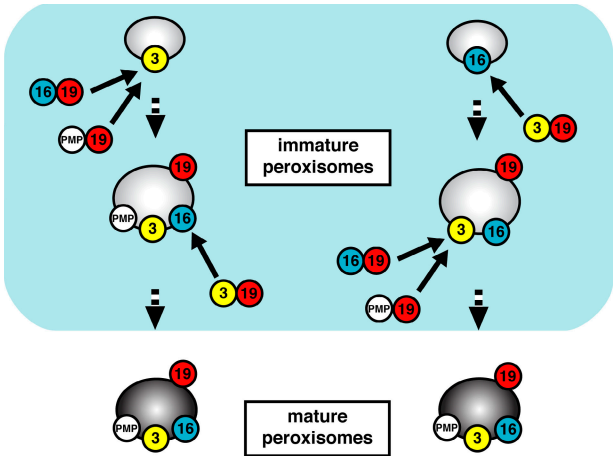

Figure 9. **A model for early stages of peroxisomal membrane biogenesis involving mutually dependent targeting of Pex3p and Pex16p.** The initial membranes harboring Pex3p or Pex16p culminate in indistinguishable, matured peroxisomes.

Materials and methods

Cell culture and antibodies

CHO-K1 and HEK293 cells were cultured as described previously (Matsumoto et al., 2003; Tsukamoto et al., 1990). Rabbit antibodies to acyl-CoA oxidase (Tsukamoto et al., 1990), Pex3p (Ghaedi et al., 2000), Pex19p (Matsuzono et al., 1999), Pex14p (Shimizu et al., 1999), Pex13p (Toyama et al., 1999), Pex16p (Honsho et al., 1998), HA (Otera et al., 2000), lactate dehydrogenase (Miyata and Fujiki, 2005), and guinea pig anti-Pex14p antibody (Mukai et al., 2002) were as described previously. Rabbit anti-human Sec61pβ antibody (Millipore) and monoclonal antibodies to c-Myc (9E10; Santa Cruz Biotechnology, Inc.), Flag (M2) (Sigma-Aldrich), HA (16B2) (Covance), α-tubulin (Clontech Laboratories, Inc.), and GFP (B2) (Santa Cruz Biotechnology, Inc.) were purchased.

Construction and transfection of epitope-tagged or EGFP-fused *PEX* cDNAs

DNA transfection into CHO cells was performed using Lipofectamine (Invitrogen; Okumoto et al., 1998). We used rat *Flag-PEX3*, rat *Flag-PEX3-HA*, rat *PEX3-EGFP*, rat *Flag-PEX3-EGFP*, rat *Flag-PEX3ΔN30-EGFP* (Ghaedi

Table I. **Synthetic oligonucleotide primers used**

Code	Sequence (5′ to 3′)	Underlined (nucleotide sequence at)
3F	CCCAAGCTTATGCTGAGATCAATGTGGAAT	1–21 of rat *PEX3*
3R	CGCGGATCCTTTCTCCAGTTGTTGGGGGGT	1096–1116 of rat *PEX3*
3(1–50)R	CGCGGATCCGGCAATGTACTCTGCAGCTTC	130–150 of rat *PEX3*
16HA2F	GCTGGATCCATGGCGTACCCCTACGATGTGCCCGATTA TGCATACCCCTACGATGTGCCCGATTATGCAATGGAGA AGCTGCGGCTCCTGGGC	Tandem *HA* (tagging to human *PEX16*)
16R	GCTCTAGATCAGCCCCAACTGTAGAAGTA	991–1000 plus a stop codon of human *PEX16*
11αHA2F	GCTGGATCCATGGCGTACCCCTACGATGTGCCCGATTA TGCATACCCCTACGATGTGCCCGATTATGCAATGGACG CCTTCACCCGCTTCACC	Tandem *HA* (tagging to human *PEX11α*)
11αR	GCTCTAGACTAACGGGTCTTCAGCTTCAT	724–741 plus a stop codon of human *PEX11α*
SSF	CGGGGTACCGCCATGGGAGCTGCTGCAAAGTTGGCGTT CGCCGTCTTTCTTATCTCTTGCTCTTCAGGTGCTATACTT GGCAGATACCCATACGATGTTCCAGATTACGCTGGATCC ATGGCG	Signal sequence of mouse activin type IIA receptor
m16R	GCTCAGCCATGTCAGCAGCTTCTGCTGGGACAGCGACAC TGGGAGTTTCTTTCTCAATTCTTTCCGTAGGATCCCGTCA TTGAG	A silence mutation in human *PEX16*
m16F	AAGCTGCTGACATGGCTGAGCGTGCTGGAGTGCGTGGAA GTCTTTATGGAAATGGGCGCT	A silence mutation in human *PEX16*

F and R, forward and reverse primers, respectively.

et al., 2000), human *HA-PEX19*, human *HA-PEX19ΔN23* (Matsuzono and Fujiki, 2006), human *Flag-PEX16-HA*, *PEX16-HA*, and *EGFP-PEX16* (Honsho et al., 1998, 2002), rat *PEX12-Myc* (Okumoto et al., 1998), human *PMP22-EGFP* (Honsho et al., 2002), human *PMP70-EGFP* (Kinoshita et al., 1998), and human *PEX26-HA* (Matsumoto et al., 2003). Epitope tagging and EGFP fusion to these peroxins did not affect the respective biological activities as in the cited references. Rat *PEX14-EGFP*, Chinese hamster *HA-PEX13*, rat *HA-PEX12*, human *HA-PEX10*, rat *HA-PEX2*, and human *HA-PEX11α* were likewise constructed as done for *PMP22-EGFP* and other *HA-PEX*s.

For rat *PEX3-Myc* and *PEX3(1–50)-Myc*, HindIII–BamHI fragments of PCR products generated using *pUcD2Hyg/Flag-RnPEX3* (Ghaedi et al., 2000) as a template with a set of primers, 3F and 3R (Table I) for *PEX3* and 3F and 3(1–50)R for *PEX3(1–50)*, were inserted into the HindIII–ApaI sites of pcDNA3.1/Zeo(+) (Invitrogen), together with the BamHI–ApaI fragment of pCMV-*6Myc*(N) (a gift from K. Tsuchida, Tokushima University, Tokushima, Japan). *SS-HA-HsPEX16* and *SS-HA-HsPEX11α* were generated by two-step PCR. For the first PCR, a set of forward and reverse primers, 16HA2F for *PEX16* (Honsho et al., 1998) and 11αHA2F for *HsPEX11α* (Abe et al., 1998), were used, and resulting fragments were used as a template for the second PCR. For the second PCR, a set of forward and reverse primers, SSF and 16R for *PEX16* and SSF and 11αR for *PEX11α*, were used. KpnI–XbaI fragment of the respective second PCR products was inserted into KpnI–XbaI sites of pcDNA3.1/Neo(+) vector (Invitrogen). To construct *HA-mPEX16*, two-step PCR was done. For the first PCR, a pair of forward and reverse primers, 16HA2F and m16R plus m16F and 16R, were used, and resulting fragments were mixed and used as a template for the second PCR. Second PCR was performed using a set of forward and reverse primers, 16HA2F and 16R. BamHI–XbaI fragment of the second PCR product was inserted into BamHI–XbaI sites in pcDNA3.1/Zeo(+) vector.

We confirmed the complementing activity of *PEX14-EGFP*, *HA-PEX13*, *HA-PEX12*, *HA-PEX10*, *HA-PEX2*, *and PEX3-Myc*, using respective *PEX*-defective mutants, and the peroxisome division activity of *HA-PEX11α* with wild-type CHO cells.

Morphological analysis

Cell fixing (Tanaka et al., 2003) and immunostaining with secondary antibodies labeled with Alexa 488, 568, and 633 (Invitrogen) were as described previously (Okumoto et al., 1998). Cells were observed under a confocal microscope (LSM 510; Carl Zeiss, Inc.). Images were acquired and analyzed with an LSM image browser (Carl Zeiss, Inc.) and ImageJ software (National Institutes of Health).

Preparation of semi-intact cells

Cells grown on 18-mm coverglass were incubated for 10 min on ice with 5% BSA in semi-intact cell buffer (SB): 0.25 M sucrose, 25 mM Hepes-KOH, pH 7.4, 2.5 mM magnesium acetate, 2.5 mM KCl, 2 mM EGTA, 0.5 μM Taxol, and protease inhibitor cocktail. After thoroughly washing with ice-cold SB, cells were incubated with 25 μg/ml digitonin in SB for 5 min at room temperature, washed three times with ice-cold SB, and incubated in SB for 30 min on ice. Lactate dehydrogenase, a cytosolic marker protein, was not discernible in the semi-permeabilized cells by immunostaining with specific antibody, hence confirming the efficient removal of the cytosol. About 80% cells were permeabilized under this condition. To assay in vitro targeting to ER membranes, CHO-K1 cells transfected with *SS-HA-PEX16* or *SS-HA-PEX11α* were permeabilized with 0.1% digitonin.

In vitro targeting assay

Semipermeabilized cells were incubated in SB with the cytosol fraction isolated from CHO-K1 cells expressing epitope-tagged Pex3p and Pex19p, washed three times with ice-cold SB, and further washed with ice-cold SB on ice for 30 min at 10-min intervals. Cells were fixed and subjected to morphological and Western blot analyses. To assess the targeting of cytosolic Pex3p stabilized by Pex19p to endogenous peroxisomes including those from CHO-K1 cells stably expressing Pex16p-HA as prepared previously (Honsho et al., 2002), targeting assay was performed at 26°C for 1 h (unless otherwise described). To evaluate the effect of ectopically and transiently expressed PMPs on the peroxisomal targeting efficiency of Pex3p–Pex19p complexes in the cytosol, targeting assay was done at 4°C for 30 min. For in vitro targeting assays using cell-free synthesized Pex3p-Myc and Pex3p(1–50)-Myc, the translation reaction mixtures were diluted with SB and incubated at 26°C for 1 h with semipermeabilized CHO-K1 cells and those expressing EGFP-Pex16p.

In vitro import assay

In vitro Pex3p-Myc import assay was performed in SB for 1 h at 26°C using cell-free synthesized Pex3p-Myc and peroxisomes isolated from CHO-K1 and CHO-K1 cells stably expressing Pex16p-HA by OptiPrep density gradient ultracentrifugation (see section below). After the reaction, peroxisomes were recovered by centrifugation at 20,000 *g* for 20 min. Import of Pex3p-Myc to peroxisomes was verified by its resistance to the alkaline treatment (Fujiki et al., 1982). Membrane and soluble fractions were separated by centrifugation at 20,000 *g* for 20 min.

Pulse-chase experiment

CHO-K1 cells were transfected with *Flag-PEX3-HA* or *Flag-PEX3-HA* plus *PEX19*. After 24-h culture, cells were pulse-labeled with 100 μCi/ml [^{35}S]methionine plus [^{35}S]cysteine (GE Healthcare) and chased for 6 h (Tsukamoto et al., 1990). Flag-Pex3p-HA was immunoprecipitated from cell lysates with rabbit anti-HA antibody (Otera et al., 2000) and analyzed

by SDS-PAGE and autoradiography with a FLA-5000 Imaging System analyzer (Fujifilm; Miyata and Fujiki, 2005). Total amounts of the immunoprecipitated Flag-Pex3p-HA were determined by immunoblotting with mouse anti-HA antibody.

OptiPrep density gradient ultracentrifugation

All steps were performed at 4°C. CHO-K1 cells and those stably expressing Pex16p-HA were homogenized in homogenize buffer (HB; 0.25 M sucrose, 20 mM Hepes-KOH, pH 7.4, 1 mM EDTA, and protease inhibitors) and centrifuged at 1,000 *g* for 10 min to yield postnuclear supernatant (PNS) fraction. Total organelle fractions were prepared by floatation on a sucrose step gradient by centrifugation in a rotor (SW55Ti; Beckman Coulter) at 55,000 rpm for 2 h. The organelle fractions were recovered from the 1.6–0.25-M interface. Peroxisomes were isolated by ultracentrifugation of the organelle fractions in 23% OptiPrep density gradient (Van Veldhoven et al., 1996), with a rotor (NVT65.2; Beckman Coulter) at 46,000 rpm for 3 h (Honsho et al., 2008). 10 1-ml fractions were collected and analyzed by SDS-PAGE and Western blotting.

RNAi

Endogenous Pex16p and Pex13p in HEK293 cells were knocked down with 100 nM siRNAs each designed for targeting human *PEX16* exon 3 and human *PEX13* exon 2 (Silencer Pre-Designed siRNA; Applied Biosystems) by transfection using siPORT Amine Transfection Agent (Applied Biosystems). As a transfection control, we used an equal amount of siRNA targeting the following sequences of *EGFP* (sense, 5′-GCAGCACGACUUCUUCAAGtt-3′; antisense, 5′-CUUGAAGAAGUCGUGCUGCtt-3′; Silencer siRNA). After 40-h incubation, cells were transfected with plasmids each for Pex3p-Myc, HA-Pex11pα, and HAmPex16p (product of a *PEX16* mutant with a silent mutation in the target sequence of siRNA) and were cultured for 12 h. To inhibit endogenous Pex19p, HEK293 cells were treated with 100 nM siRNA designed for targeting human *PEX19* (ON-TARGET*plus* SMARTpool siRNA; Thermo Fisher Scientific) twice at a 24-h interval using DharmaFECT1 transfection reagent (Thermo Fisher Scientific). As a transfection control, we used an equal amount of control siRNA (siCONTROL Non-targeting siRNA pool; Thermo Fisher Scientific). At 48 h after the first siRNA treatment, cells were transfected with plasmids each for Pex3p-Myc and Pex3p(1–50)-Myc and were cultured for 24 h.

Other methods

In vitro transcription/translation (Miyata and Fujiki, 2005), in vitro binding assays (Otera et al., 2000) using in vitro synthesized Pex3p-Myc, Pex3p(1–50)-Myc, Flag-Pex16p-HA, and Myc (pCMV-*6Myc*(N) vector product), and subcellular fractionation and Western blotting (Otera et al., 2000) were done as described previously. Immunoprecipitation from cytosol fractions was done with anti-HA antibody or preimmune sera after the dilution with an equal volume of 1% digitonin, 20 mM Hepes-KOH, pH 7.4, 0.3 M NaCl, 1 mM EDTA, and protease inhibitors.

Online supplemental material

Fig. S1 (supplement to Fig. 3) shows that Pex16p recruits Pex3p–Pex19p complexes. Fig. S2 shows that the elevated level of membrane-integrated Pex16p enhances the efficiency of Pex19p-mediated Pex3p targeting. Fig. S3 shows that Pex3p targeted to Pex16p is integrated into the peroxisomal membranes in a temperature-dependent and ATP-independent manner. Fig. S4 shows that the full-length Pex16p is required for recruiting cytosolic Pex3p–Pex19p complexes to peroxisomes. Online supplemental material is available at http://www.jcb.org/cgi/content/full/jcb.200806062/DC1.

We thank M. Nishi for preparing figures, N. Thomas for comments, K. Hosoi for the help partly in ultracentrifugation on a OptiPrep density gradient, and the other members of the Fujiki laboratory for discussions.

This work was supported in part by Solution Oriented Research for Science and Technology and Core Research for Evolutional Science and Technology grants (to Y. Fujiki) from the Science and Technology Agency of Japan; Grants-in-Aid for Scientific Research (to Y. Fujiki); grant of the National Project on Protein Structural and Functional Analyses (to Y. Fujiki); the 21st Century Centers of Excellence (COE) and Global COE Programs from the Ministry of Education, Culture, Sports, Science and Technology of Japan; and grants from the Japan Foundation for Applied Enzymology and the Takeda Foundation for Biomedical Research.

Submitted: 10 June 2008
Accepted: 2 December 2008

References

Abe, I., K. Okumoto, S. Tamura, and Y. Fujiki. 1998. Clofibrate-inducible, 28-kDa peroxisomal integral membrane protein is encoded by *PEX11*. *FEBS Lett.* 431:468–472.

Eitzen, G.A., R.K. Szilard, and R.A. Rachubinski. 1997. Enlarged peroxisomes are present in oleic acid–grown *Yarrowia lipolytica* overexpressing the *PEX16* gene encoding an intraperoxisomal peripheral membrane peroxin. *J. Cell Biol.* 137:1265–1278.

Fang, Y., J.C. Morrell, J.M. Jones, and S.J. Gould. 2004. PEX3 functions as a PEX19 docking factor in the import of class I peroxisomal membrane proteins. *J. Cell Biol.* 164:863–875.

Fransen, M., T. Wylin, C. Brees, G.P. Mannaerts, and P.P. Van Veldhoven. 2001. Human Pex19p binds peroxisomal integral membrane proteins at regions distinct from their sorting sequences. *Mol. Cell. Biol.* 21:4413–4424.

Fujiki, Y., A.L. Hubbard, S. Fowler, and P.B. Lazarow. 1982. Isolation of intracellular membranes by means of sodium carbonate treatment: application to endoplasmic reticulum. *J. Cell Biol.* 93:97–102.

Fujiki, Y., Y. Matsuzono, T. Matsuzaki, and M. Fransen. 2006a. Import of peroxisomal membrane proteins: the interplay of Pex3p- and Pex19p-mediated interactions. *Biochim. Biophys. Acta.* 1763:1639–1646.

Fujiki, Y., K. Okumoto, N. Kinoshita, and K. Ghaedi. 2006b. Lessons from peroxisome-deficient Chinese hamster ovary (CHO) cell mutants. *Biochim. Biophys. Acta.* 1763:1374–1381.

Ghaedi, K., S. Tamura, K. Okumoto, Y. Matsuzono, and Y. Fujiki. 2000. The peroxin Pex3p initiates membrane assembly in peroxisome biogenesis. *Mol. Biol. Cell.* 11:2085–2102.

Goette, K., W. Girzalsky, M. Linkert, E. Baumgart, S. Kammerer, W.-H. Kunau, and R. Erdmann. 1998. Pex19p, a farnesylated protein essential for peroxisome biogenesis. *Mol. Cell. Biol.* 18:616–628.

Heiland, I., and R. Erdmann. 2005. Biogenesis of peroxisomes: topogenesis of the peroxisomal membrane and matrix proteins. *FEBS J.* 272:2362–2372.

Hettema, E.H., W. Girzalsky, M. van den Berg, R. Erdmann, and B. Distel. 2000. *Saccharomyces cerevisiae* Pex3p and Pex19p are required for proper localization and stability of peroxisomal membrane proteins. *EMBO J.* 19:223–233.

Hoehfeld, J., M. Veenhuis, and W.H. Kunau. 1991. PAS3, a *Saccharomyces cerevisiae* gene encoding a peroxisomal integral membrane protein essential for peroxisome biogenesis. *J. Cell Biol.* 114:1167–1178.

Hoepfner, D., D. Schildknegt, I. Braakman, P. Philippsen, and H.F. Tabak. 2005. Contribution of the endoplasmic reticulum to peroxisome formation. *Cell.* 122:85–95.

Honsho, M., S. Tamura, N. Shimozawa, Y. Suzuki, N. Kondo, and Y. Fujiki. 1998. Mutation in *PEX16* is causal in the peroxisome-deficient Zellweger syndrome of complementation group D. *Am. J. Hum. Genet.* 63:1622–1630.

Honsho, M., T. Hiroshige, and Y. Fujiki. 2002. The membrane biogenesis peroxin Pex16p: topogenesis and functional roles in peroxisomal membrane assembly. *J. Biol. Chem.* 277:44513–44524.

Honsho, M., Y. Yagita, N. Kinoshita, and Y. Fujiki. 2008. Isolation and characterization of mutant animal cell line defective in alkyl-dihydroxyacetonephosphate synthase: localization and transport of plasmalogens to post-Golgi compartment. *Biochim. Biophys. Acta.* In press.

Jones, J.M., J.C. Morrell, and S.J. Gould. 2004. PEX19 is a predominantly cytosolic chaperone and import receptor for class 1 peroxisomal membrane proteins. *J. Cell Biol.* 164:57–67.

Kammerer, S., A. Holzinger, U. Welsch, and A.A. Roscher. 1998. Cloning and characterization of the gene encoding the human peroxisomal assembly protein Pex3p. *FEBS Lett.* 429:53–60.

Kim, P.K., R.T. Mullen, U. Schumann, and J. Lippincott-Schwartz. 2006. The origin and maintenance of mammalian peroxisomes involves a de novo PEX16-dependent pathway from the ER. *J. Cell Biol.* 173:521–532.

Kinoshita, N., K. Ghaedi, N. Shimozawa, R.J.A. Wanders, Y. Matsuzono, T. Imanaka, K. Okumoto, Y. Suzuki, N. Kondo, and Y. Fujiki. 1998. Newly identified Chinese hamster ovary cell mutants are defective in biogenesis of peroxisomal membrane vesicles (peroxisomal ghosts), representing a novel complementation group in mammals. *J. Biol. Chem.* 273:24122–24130.

Kragt, A., T. Voorn-Brouwer, M. van den Berg, and B. Distel. 2005. ER-directed Pex3p routes to peroxisomes and restores peroxisome formation in a *Saccharomyces cerevisiae pex3Δ* strain. *J. Biol. Chem.* 280:34350–34357.

Lazarow, P.B., and Y. Fujiki. 1985. Biogenesis of peroxisomes. *Annu. Rev. Cell Biol.* 1:489–530.

Manders, E.M.M., F.J. Verbeek, and J.A. Aten. 1993. Measurement of co-localization of objects in dual-colour confocal images. *J. Microsc.* 169:375–382.

Matsumoto, N., S. Tamura, and Y. Fujiki. 2003. The pathogenic peroxin Pex26p recruits the Pex1p-Pex6p AAA ATPase complexes to peroxisomes. *Nat. Cell Biol.* 5:454–460.

Matsuzaki, T., S. Hanai, H. Kishi, Z. Liu, Y. Bao, A. Kikuchi, K. Tsuchida, and H. Sugino. 2002. Regulation of endocytosis of activin type II receptors by a novel PDZ protein through Ral/Ral-binding protein 1-dependent pathway. *J. Biol. Chem.* 277:19008–19018.

Matsuzono, Y., and Y. Fujiki. 2006. *In vitro* transport of membrane proteins to peroxisomes by shuttling receptor Pex19p. *J. Biol. Chem.* 281:36–42.

Matsuzono, Y., N. Kinoshita, S. Tamura, N. Shimozawa, M. Hamasaki, K. Ghaedi, R.J.A. Wanders, Y. Suzuki, N. Kondo, and Y. Fujiki. 1999. Human *PEX19*: cDNA cloning by functional complementation, mutation analysis in a patient with Zellweger syndrome and potential role in peroxisomal membrane assembly. *Proc. Natl. Acad. Sci. USA.* 96:2116–2121.

Matsuzono, Y., T. Matsuzaki, and Y. Fujiki. 2006. Functional domain mapping of peroxin Pex19p: interaction with Pex3p is essential for function and translocation. *J. Cell Sci.* 119:3539–3550.

Miyata, N., and Y. Fujiki. 2005. Shuttling mechanism of peroxisome targeting signal type 1 receptor, Pex5: ATP-independent import and ATP-dependent export. *Mol. Cell. Biol.* 25:10822–10832.

Mukai, S., K. Ghaedi, and Y. Fujiki. 2002. Intracellular localization, function, and dysfunction of the peroxisome-targeting signal type 2 receptor, Pex7p, in mammalian cells. *J. Biol. Chem.* 277:9548–9561.

Muntau, A.C., P.U. Mayerhofer, B.C. Paton, S. Kammerer, and A.A. Roscher. 2000. Defective peroxisome membrane synthesis due to mutations in human *PEX3* causes Zellweger syndrome, complementation group G. *Am. J. Hum. Genet.* 67:967–975.

Okumoto, K., N. Shimozawa, A. Kawai, S. Tamura, T. Tsukamoto, T. Osumi, H. Moser, R.J.A. Wanders, Y. Suzuki, N. Kondo, and Y. Fujiki. 1998. *PEX12*, the pathogenic gene of group III Zellweger syndrome: cDNA cloning by functional complementation on a CHO cell mutant, patient analysis, and characterization of Pex12p. *Mol. Cell. Biol.* 18:4324–4336.

Otera, H., T. Harano, M. Honsho, K. Ghaedi, S. Mukai, A. Tanaka, A. Kawai, N. Shimizu, and Y. Fujiki. 2000. The mammalian peroxin Pex5pL, the longer isoform of the mobile PTS1-transporter, translocates Pex7p-PTS2 protein complex into peroxisomes via its initial docking site, Pex14p. *J. Biol. Chem.* 275:21703–21714.

Platta, H.W., and R. Erdmann. 2007. Peroxisomal dynamics. *Trends Cell Biol.* 17:474–484.

Sacksteder, K.A., J.M. Jones, S.T. South, X. Li, Y. Liu, and S.J. Gould. 2000. PEX19 binds multiple peroxisomal membrane proteins, is predominantly cytoplasmic, and is required for peroxisome membrane synthesis. *J. Cell Biol.* 148:931–944.

Schlueter, A., R. Ripp, S. Fourcade, J.L. Mandel, O. Poch, and A. Pujol. 2006. The evolutionary origin of peroxisomes: an ER-peroxisome connection. *Mol. Biol. Evol.* 23:838–845.

Shimizu, N., R. Itoh, Y. Hirono, H. Otera, K. Ghaedi, K. Tateishi, S. Tamura, K. Okumoto, T. Harano, S. Mukai, and Y. Fujiki. 1999. The peroxin Pex14p: cDNA cloning by functional complementation on a Chinese hamster ovary cell mutant, characterization, and functional analysis. *J. Biol. Chem.* 274:12593–12604.

South, S.T., and S.J. Gould. 1999. Peroxisome synthesis in the absence of preexisting peroxisomes. *J. Cell Biol.* 144:255–266.

South, S.T., K.A. Sacksteder, X. Li, Y. Liu, and S.J. Gould. 2000. Inhibitors of COPI and COPII do not block *PEX3*-mediated peroxisome synthesis. *J. Cell Biol.* 149:1345–1360.

Tam, Y.Y.C., A. Fagarasanu, M. Fagarasanu, and R.A. Rachubinski. 2005. Pex3p initiates the formation of a preperoxisomal compartment from a subdomain of the endoplasmic reticulum in *Saccharomyces cerevisiae. J. Biol. Chem.* 280:34933–34939.

Tanaka, A., K. Okumoto, and Y. Fujiki. 2003. cDNA cloning and characterization of the third isoform of human peroxin Pex11p. *Biochem. Biophys. Res. Commun.* 300:819–823.

Titorenko, V.I., and R.A. Rachubinski. 1998. Mutants of the yeast *Yarrowia lipolytica* defective in protein exit from the endoplasmic reticulum are also defective in peroxisome biogenesis. *Mol. Cell. Biol.* 18:2789–2803.

Titorenko, V.I., D.M. Ogrydziak, and R.A. Rachubinski. 1997. Four distinct secretory pathways serve protein secretion, cell surface growth, and peroxisome biogenesis in the yeast *Yarrowia lipolytica. Mol. Cell. Biol.* 17:5210–5226.

Toyama, R., S. Mukai, A. Itagaki, S. Tamura, N. Shimozawa, Y. Suzuki, N. Kondo, R.J.A. Wanders, and Y. Fujiki. 1999. Isolation, characterization, and mutation analysis of *PEX13*-defective Chinese hamster ovary cell mutants. *Hum. Mol. Genet.* 8:1673–1681.

Tsukamoto, T., S. Yokota, and Y. Fujiki. 1990. Isolation and characterization of Chinese hamster ovary cell mutants defective in assembly of peroxisomes. *J. Cell Biol.* 110:651–660.

van den Bosch, H., R.B.H. Schutgens, R.J.A. Wanders, and J.M. Tager. 1992. Biochemistry of peroxisomes. *Annu. Rev. Biochem.* 61:157–197.

Van Veldhoven, P.P., E. Baumgart, and G.P. Mannaerts. 1996. Iodixanol (Optiprep), an improved density gradient medium for the iso-osmotic isolation of rat liver peroxisomes. *Anal. Biochem.* 237:17–23.